Available online at www.sciencedirect.com
ScienceDirect
International Journal of Mass Spectrometry 265 (2007) 251–260
International Journal of Mass Spectrometry
www.elsevier.com/locate/ijms

Unimolecular chemistry of metal ion-coordinated α-dipeptide radicals

Francesco Pingitore [a,1], Christian Bleiholder [b], Béla Paizs [b], Chrys Wesdemiotis [a,*]

[a] *Department of Chemistry, The University of Akron, Akron, OH 44325-3601, USA*
[b] *Protein Analysis Facility, German Cancer Research Center, Heidelberg, Germany*

Received 1 January 2007; received in revised form 6 February 2007; accepted 20 February 2007
Available online 23 February 2007

Dedicated to Professor Jean H. Futrell for his inspiring and seminal work on gas phase ion chemistry and physics.

Abstract

The Li^+ complexes of the isomeric α-dipeptide radicals $H_2N{-}^{\bullet}CH{-}C(=O){-}NH{-}CH_2{-}COOH$ ($^{\bullet}$GlyGly) and $H_2N{-}CH_2{-}C(=O){-}NH{-}^{\bullet}CH{-}COOH$ (GlyGly$^{\bullet}$) are formed in the gas phase from the isomeric complexes $[PheGly + Li]^+$ and $[GlyPhe + Li]^+$, respectively, via homolytic cleavage of the corresponding benzyl side chains. The isomers undergo distinctively different reactions upon collisionally activated dissociation (CAD) and, hence, represent unique, non-interconverting species. The investigation of deuterated isotopomers and of dipeptide radicals with Ala residues permits complete elucidation of the dissociation pathways of the radical complexes. The majority of reactions observed are promoted by the radical site, with the location of the unpaired electron playing an important role in the types of reactions taking place. Analogous differences are found for dilithiated complexes of $^{\bullet}$GlyGly and GlyGly$^{\bullet}$, in which the COOH termini are derivatized to COO^-Li^+ salt bridges. Density functional theory calculations confirm that the lithiated and dilithiated α-dipeptide radicals have distonic character; the radical is largely localized on the N- or C-terminal α-C atom and the charge is largely localized on the metal ions. In the most stable conformers, the Li^+ ion(s) are bound between the amide carbonyl and C-terminal carbonyl (or carboxylate) groups. Theory predicts a higher thermodynamic stability for the complexes of the N-terminal radical $^{\bullet}$GlyGly, as reflected by the significantly higher yield, with which these complexes are formed (from their PheGly precursors), compared to the GlyGly$^{\bullet}$ complexes.

Keywords: Peptide radicals; Distonic ions; Salt bridges; Tandem MS; Metalated peptides

1. Introduction

Protein radicals with the unpaired electron at the α-C atom of a glycyl residue have been implicated as transient or stable intermediates in several biological processes, both deleterious and beneficial [1–4]. Radiolytically generated HO$^{\bullet}$ radicals attack the protein backbone preferentially at glycyl positions, because the resulting α-glycyl radicals are not sterically hindered (no presence of side chains) and, thus, can easily attain a planar resonance-stabilized conformation [5]. Backbone radicals produced this way may fragment or cross-link, thereby impeding protein function and initiating pathogenic processes, such as cancer, inflammatory disease or Alzheimer's [6]. On the other hand, it is well established that proteins with α-glycyl radical sites can also be involved in essential biocatalysis [2,3]. This is true for anaerobic ribonucleotide reductase and pyruvate–formate lyase, both of which carry glycyl radicals, introduced post-translationally, at positions 681 and 734, respectively [7–10].

Protein backbone radicals have mainly been examined by electron paramagnetic resonance (EPR) spectroscopy [1,4–10]. Their chemical properties have remained largely unknown due to their transient nature. The intrinsic dissociations and biomolecular reactions of these species are of fundamental interest, as they could provide the insight needed for a better assessment of their in vivo reactivity. Mass spectrometry offers a convenient means for the isolation and the study of transient intermediates, if these are charged. Kenttämaa and coworkers [11–16] and, more recently, our group [17–21] have demonstrated that organic radicals containing inert charges, including alkali metal ion or quaternary pyridinium sites, primarily react at their radical centers. Such systems can therefore serve as templates for the investigation of the gas-phase chemistry of the corresponding neutral radicals. This approach is used here to characterize

* Corresponding author. Tel.: +1 330 972 7699; fax: +1 330 972 7370.
E-mail address: wesdemiotis@uakron.edu (C. Wesdemiotis).
[1] Present address: Berkeley Center for Synthetic Biology, University of California, Berkeley, CA 94720, USA.

1387-3806/$ – see front matter © 2007 Elsevier B.V. All rights reserved.
doi:10.1016/j.ijms.2007.02.029

in detail the intrinsic chemistry of dipeptides carrying α-glycyl radicals, which represent simple models for the more complex protein backbone radicals. The species studied contain an unpaired electron either in N- or C-terminal position and are ionized by Li^+ ions, i.e. they have the connectivity $[^\bullet GlyXxx + Li]^+$ or $[XxxGly^\bullet + Li]^+$, where $Gly^\bullet$ designates the α-glycyl residue and Xxx = Gly or Ala. The corresponding dilithiated complexes, in which the –COOH termini are derivatized to $–COO–Li^+$, are also investigated in order to determine the influence of salt bridges on radical reactivity. We recently showed that such radical ions can be generated by collisionally activated dissociation (CAD) of mono- or dilithiated dipeptides containing an aromatic amino acid residue at the position where the $Gly^\bullet$ radical is to be introduced [20]. This method complements the synthetic procedure recently introduced by Siu et al. [22], in which radical ions of complete peptides (they have one more H atom than the α-peptide radicals studied here) are prepared via gas-phase redox reactions from ternary complexes of a multiply charged transition metal ion, the peptide of interest and an auxiliary multidentate ligand [22–25].

2. Experimental

2.1. Mass spectrometry

Mass spectrometry experiments were conducted on a Waters/Micromass AutoSpec-Q tandem mass spectrometer of E_1BE_2hQ geometry (Waters, Beverly, MA), where E, B, h and Q designate an electrostatic analyzer, magnetic sector, hexapole collision cell and quadrupole mass filter, respectively. Only the sector portion of the instrument (E_1BE_2) was utilized in this study. Dipeptides AaaXxx or XxxAaa (Aaa = aromatic amino acid; Xxx = Gly or Ala) were ionized by fast atom bombardment (FAB), using 1–2 μL of oversaturated solutions that were prepared by adding each dipeptide and lithium trifluoroacetate to thioglycerol in a ratio of 5:1. FAB ionization of these solutions produced monolithiated $[AaaXxx + Li]^+$ or $[XxxAaa + Li]^+$ complexes as well as dilithiated $[AaaXxx - H + 2Li]^+$ or $[XxxAaa - H + 2Li]^+$ complexes [20,21]. After acceleration to 8 keV, these ions were subjected to CAD with He in the field-free region following the ion source (in front of E_1) to detach the aromatic side chain of Aaa and generate the corresponding dipeptide radicals, viz. $[^\bullet GlyXxx + Li]^+$, $[XxxGly^\bullet + Li]^+$, $[^\bullet GlyXxx - H + 2Li]^+$ or $[XxxGly^\bullet - H + 2Li]^+$, respectively. The charged radicals were transmitted to the third field-free region (between B and E_2) for renewed CAD with Ar. The MS^3 fragments produced this way were dispersed by E_2 (kinetic energy scans) and detected in the corresponding CAD (MS^3) mass spectra. Control CAD (MS^2) spectra of the mono- and dilithiated peptides were acquired by transmitting these ions through E_1B, inducing their fragmentation in the third field-free region via CAD with Ar and mass-analyzing the resulting fragments by scanning E_2. Approximately, 100 scans were summed to obtain spectra with a good signal/noise ratio. The dipeptides were purchased from Bachem (King of Prussia, PA) and thioglycerol and trifluoroacetate from Aldrich (Milwaukee, WI).

For H/D exchange, ∼10 mg of the dipeptide was dissolved in 1 mL of D_2O that was acidified by ∼5 μL of D_2SO_4. The solution was stirred overnight. A few microliters of the solution were mixed with an equal volume of thioglycerol for FAB ionization. During the treatment with D_2O/D_2SO_4, all exchangeable protons are replaced with deuteria; there are four exchangeable protons in the lithiated complexes and three in the dilithiated ones. Upon mixing with thioglycerol, back exchange is possible, as the FAB spectra revealed mixtures of isotopomers. For $[GlyPhe + Li]^+$, $[PheGly - H + 2Li]^+$ and $[PheGly - H + 2Li]^+$, the isotopomers with all labile H atoms exchanged with D atoms (d_4, d_3 and d_3, respectively) were sufficiently intense for the acquisition of MS^3 spectra. For $[PheGly + Li]^+$, the isotopomer with only three D atoms was more intense than that with four D atoms; only the former ion could be subjected to MS^3. Based on the procedure of H/D exchange, the most likely deuterium replaced by hydrogen upon mixing with thioglycerol is the carboxylic H atom. Hence, d_3-$[^\bullet GlyGly + Li]^+$ should mainly be composed of the $D_2N–^\bullet CH–C(=O)–ND–CH_2–COOH$ isotopomer of $^\bullet GlyGly$.

2.2. Calculations

A recently developed conformational search engine devised originally to deal with protonated peptides was modified and subsequently used to scan the potential energy surface (PES) of lithiated and dilithiated $^\bullet GlyGly$ and $GlyGly^\bullet$. Calculations started with molecular dynamics simulations on charge solvated (CS) and salt-bridge (SB) species of the above ions using the Insight II program (Biosym Technologies, San Diego, USA) in conjunction with the AMBER force field. During the dynamics calculations, simulated annealing techniques were used to produce candidate structures for further refinement, applying full geometry optimization with the AMBER force field. The optimized structures were then analyzed by a conformer family search program, developed at Heidelberg, which is able to group optimized structures into families with similar structural features. The most stable species in the families were then fully optimized at the HF/3-21G, B3LYP/6-31G(d) and B3LYP/6-31 + G(d,p) levels. The conformer families were regenerated at each computational level. For the energetically most preferred structures, frequency calculations were performed at the B3LYP/6-31G(d) level of theory. Relative energies were calculated by comparing the B3LYP/6-31 + G(d,p) total energies, corrected for zero-point vibrational energy (ZPE) determined at the B3LYP/6-31G(d) level, to that of the global minimum of a given ion. The Gaussian set of programs [26] was used for all ab initio and density functional theory calculations.

3. Results and discussion

3.1. Generation of the metalated dipeptide radicals

Dipeptides containing a Phe or Trp residue in N- or C-terminal position were used to generate the dipeptide radicals. As shown in Fig. 1, high energy CAD of the complexes $[PheGly + Li]^+$ and $[GlyPhe + Li]^+$ partly causes homolytic

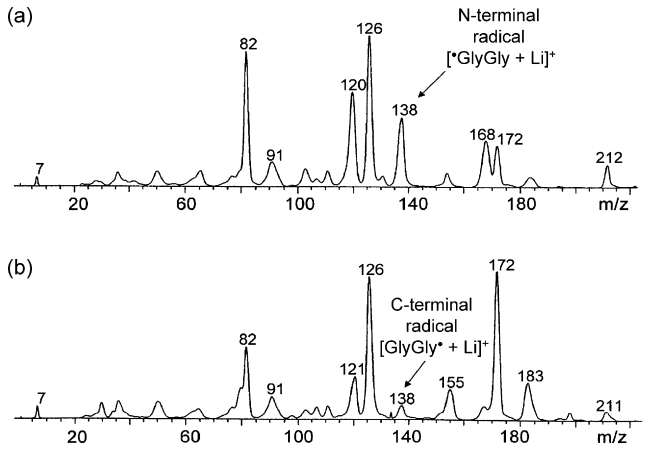

Fig. 1. CAD (MS^2) mass spectra of (a) $[PheGly + Li]^+$ and (b) $[GlyPhe + Li]^+$ (both at *m/z* 229). The numbers on top of the peaks give the corresponding mass-to-charge ratios.

cleavage of benzyl radicals ($PhCH_2^{\bullet}$), giving rise to the lithiated dipeptide radicals $[^{\bullet}GlyGly + Li]^+$ and $[GlyGly^{\bullet} + Li]^+$, respectively (both at *m/z* 138). Similarly, the Li^+ complex of $^{\bullet}$GlyAla (*m/z* 152) can be generated from the Li^+ complexes of PheAla and TrpAla. The Li^+ complex of AlaGly$^{\bullet}$ could not be produced in sufficient intensity or purity from $[AlaPhe + Li]^+$ or $[AlaTrp + Li]^+$ for the acquisition of usable MS^3 spectra.

The dilithiated complexes $[AaaXxx - H + 2Li]^+$ and $[XxxAaa - H + 2Li]^+$, where Aaa = Phe or Trp and Xxx = Gly or Ala, served as precursors for the production via CAD of the dilithiated radicals $[^{\bullet}GlyXxx - H + 2Li]^+$ and $[XxxGly^{\bullet} - H + 2Li]^+$, respectively. The CAD spectra of $[PheGly - H + 2Li]^+$ and $[GlyPhe - H + 2Li]^+$ are presented in Fig. 2 as representative examples. It is evident from Figs. 1 and 2 that the dilithiated peptides undergo more efficiently loss of their aromatic side chain upon CAD, yielding higher fluxes of dipeptide radical ions than the corresponding monolithiated systems. Generally, a higher abundance is observed for the

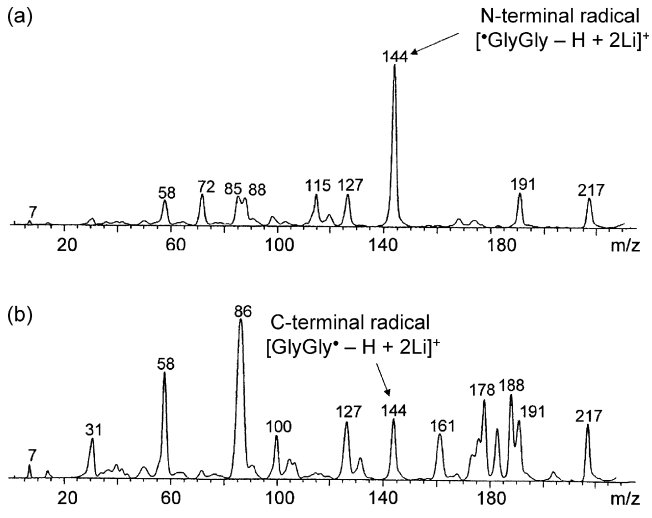

Fig. 2. CAD (MS^2) mass spectra of (a) $[PheGly - H + 2Li]^+$ and (b) $[GlyPhe - H + 2Li]^+$ (both at *m/z* 235). The numbers on top of the peaks give the corresponding mass-to-charge ratios.

charged radical if the unpaired electron resides at the N-terminal residue. These trends suggest that a radical site in N-terminal position and a salt bridge (in the dilithiated systems) increase the stability of α-peptide radicals (vide infra).

3.2. Calculated structures of the glycylglycine complexes

The most stable structures predicted by density functional theory (DFT) for lithiated and dilithiated $^{\bullet}$GlyGly and GlyGly$^{\bullet}$ are shown in Figs. 3 and 4. Because of the large number of different isomers and conformers obtained during the scan of the PES of these radical ions, full optimization and energy minimization were performed only on the lower energy species (those lying within ~30 kJ/mol of most stable isomers). Higher energy structures (within the 30 kJ/mol energy window) are described only if they show a specific type of interaction which is not present in the energetically most favored species.

Structures involving charge solvation are denoted by CS and those containing a salt bridge by SB. The various conformer families are abbreviated using the nomenclature of Dunbar [27], which provides information about the most important interactions between the metal ion(s) and the functionalities of the investigated peptide radicals. For example, 'CS O/OA' for $[^{\bullet}GlyGly + Li]^+$ (Fig. 3) denotes a charge solvation structure with Li^+ bound to the COOH carbonyl oxygen (O) and amide oxygen (OA), while 'SB OA/OC OC/OC' for $[GlyGly^{\bullet} - H + 2Li]^+$ (Fig. 4) denotes a salt bridge structure with one Li^+ bound between the amide oxygen (OA) and one carboxylate oxygen (OC) and the other Li^+ bound between the two carboxylate oxygens (OC). The amine nitrogen and amide nitrogen binding sites of $^{\bullet}$GlyGly and GlyGly$^{\bullet}$ are designated by N and NA, respectively.

The most stable isomers of lithiated $^{\bullet}$GlyGly as well as GlyGly$^{\bullet}$ result from charge solvation of the metal ion by the carbonyl oxygens of the amide and carboxyl groups (Fig. 3). These complexes are additionally stabilized by hydrogen bonds, which can develop between the amide oxygen and one amine proton in $[^{\bullet}GlyGly + Li]^+$, and between the amine nitrogen and amide proton in $[GlyGly^{\bullet} + Li]^+$. The second most stable structure found for lithiated $^{\bullet}$GlyGly contains a COO–Li^+ salt bridge, an O-protonated amide group and hydrogen bonds between the amide group and the two termini. No low energy lying salt bridge isomer was found for lithiated GlyGly$^{\bullet}$; with this radical, the second most stable complex results from Li^+ solvation between the amine nitrogen and amide oxygen, stabilized by a hydrogen bond between the amide proton and the C-terminal carbonyl oxygen.

The most stable isomers of dilithiated $^{\bullet}$GlyGly and GlyGly$^{\bullet}$ carry a COO–Li^+ salt bridge, with the second Li^+ ion bound between a carboxylate oxygen and the amide oxygen (Fig. 4). As with the monolithiated species, these structures are stabilized further by hydrogen bonds between the N-terminus and the amide group. No other low energy structure exists for $[^{\bullet}GlyGly - H + 2Li]^+$. In contrast, several isomeric, low-energy structures were found for $[GlyGly^{\bullet} - H + 2Li]^+$, having one Li^+ ion coordinated between the N-terminal amine nitrogen and the amide group, and the other Li^+ ion bound either at a deproto-

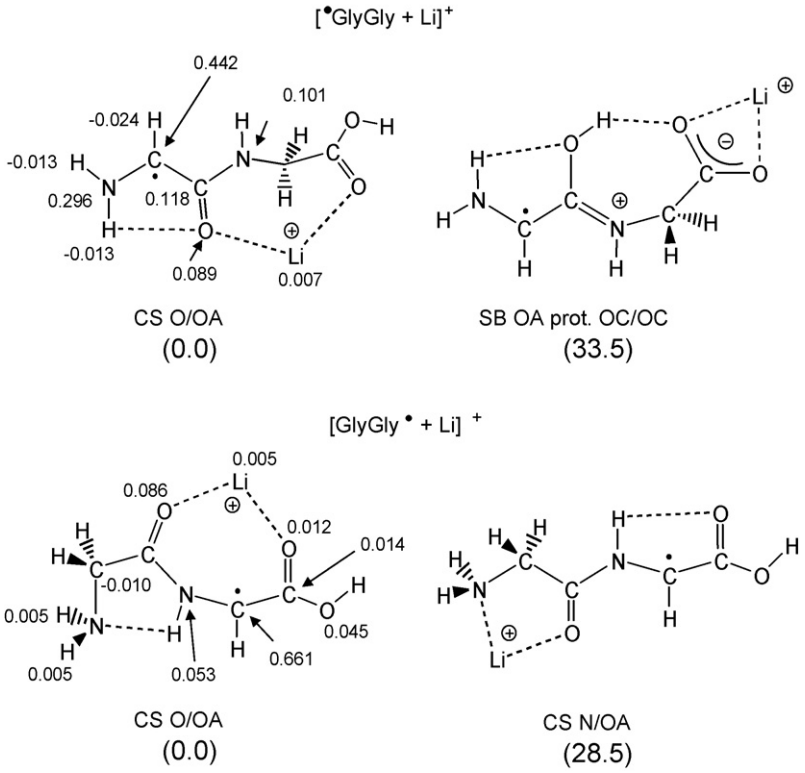

Fig. 3. Most stable isomers of the Li^+ complexes of •GlyGly (top) and GlyGly• (bottom), predicted at the B3LYP level of density functional theory. See text for the abbreviations used to describe coordination features. The numbers next to the atoms give atomic spin densities (no values are given for densities <0.001). The numbers in parenthesis are relative energies in kJ/mol. The charges on Li in the most stable isomers of •GlyGly and GlyGly• are 0.586 and 0.601, respectively.

nated carboxylate or a deprotonated amide salt bridge (Fig. 4). It is worth mentioning that metal ion coordination at the N-terminus is not favored if the unpaired electron resides at the α-C atom of the N-terminal residue; this is true for both the mono- as well as the dilithiated complexes.

The B3LYP/6-31 + G(d,p) Mulliken atomic spin densities of the most stable mono- and dilithiated geometries (Figs. 3 and 4) indicate that the radical resides largely at the α-C atom of either the N- or the C-terminal residue. Conversely, the positive charge is primarily localized on the metal ion(s) (see legends of Figs. 3 and 4). Hence, these complexes have distonic character.

Radical sites are best stabilized if they are simultaneously surrounded by electron-donating and electron-withdrawing groups (capto-dative substitution pattern [1]). This feature is present in •GlyGly. As a result of such capto-dative substitution, the unpaired electron in lithiated and dilithiated •GlyGly is partly delocalized into the amine nitrogen, $H_2N–•CH–CO– \leftrightarrow H_2N^+•–^-CH–CO–$; this resonance increases the positive charge at the amine nitrogen, explaining why •GlyGly cannot form low energy mono- or dilithiated complexes in which the (positively charged) metal ion is bound at the (partly positively charged) N-terminal amine group. The DFT calculations also predict that the most stable structure of $[•GlyGly + Li]^+$ (CS O/OA) is 28 kJ/mol more stable than the most stable structure of $[GlyGly• + Li]^+$ (CS O/OA). Similarly, the most stable $[•GlyGly - H + 2Li]^+$ complex is predicted to lie 39 kJ/mol lower in energy than the most stable $[GlyGly• - H + 2Li]^+$ complex (both SB OA/OC OC/OC). The consistently higher thermodynamic stability of the N-terminal radical complexes (i.e. those bearing the radical site at the N-terminal α-C atom) reflects the better stabilization of the unpaired electron at the N-terminal α-site (vide supra) and the increased electron density of the binding sites near the C-terminus (where the metal ions preferentially attach) when the unpaired electron is not located at the C-terminal α-C atom.

3.3. Unimolecular chemistry of the monolithiated N- and C-terminal dipeptide radicals

With both $[PheGly + Li]^+$ and $[GlyPhe + Li]^+$, CAD leads to the formation of product ions at *m/z* 138 (Fig. 1), corresponding to the isomeric dipeptide radical complexes $[•GlyGly + Li]^+$ and $[GlyGly• + Li]^+$, respectively (Fig. 3). These metalated distonic ions were characterized by a further stage of CAD experiments. The resulting MS^3 (CAD/CAD) spectra, depicted in Fig. 5, unequivocally prove that the dilithiated •GlyGly/GlyGly• isomers have unique unimolecular chemistries and, hence, distinct, non-interconverting structures. The reactions observed indicate that individual dissociation channels, promoted by the location of the radical site (vide infra), are more competitive than isomerization. A loss of 17 u (*m/z* 121) is observed from the $[GlyGly• + Li]^+$ species exclusively, along with product ions at *m/z* 82 and 80 (Fig. 5b); meanwhile, in the MS^3 spectrum of $[•GlyGly + Li]^+$, significant peaks are observed at *m/z* 82 and 79 (Fig. 5a). In order to establish the structures of the major fragments, additional MS^3 experiments with deuterated isotopomers

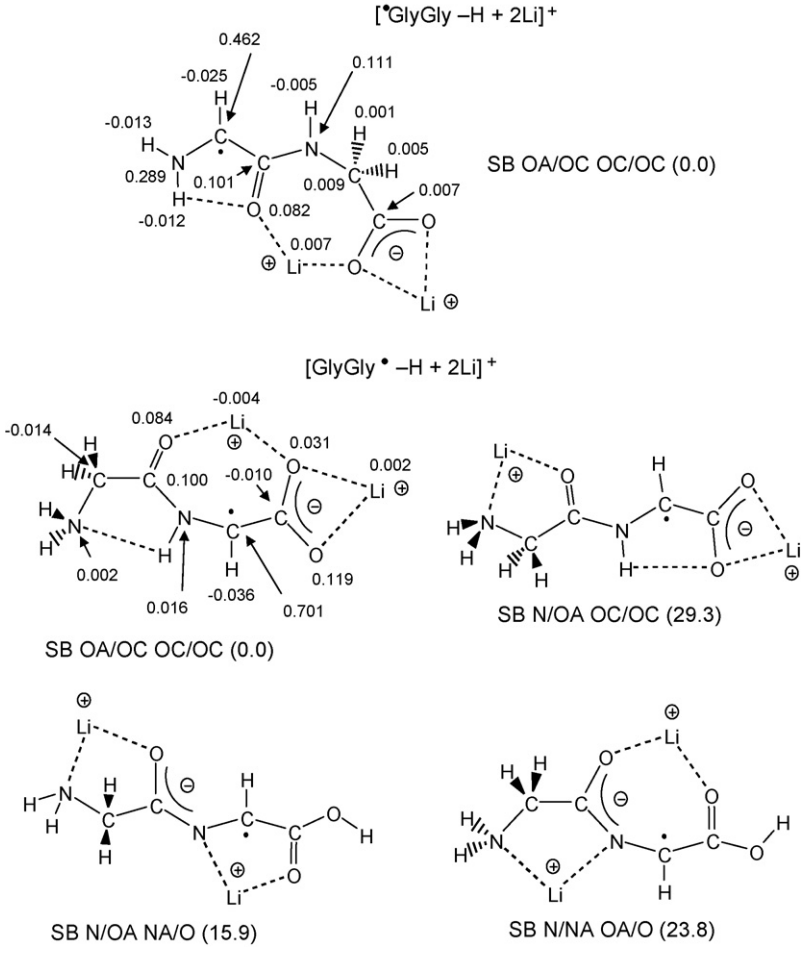

Fig. 4. Most stable isomers of dilithiated •GlyGly (top) and GlyGly• (center and bottom), predicted at the B3LYP level of density functional theory. See text for the abbreviations used to describe coordination features. The numbers next to the atoms give atomic spin densities (no values are given for densities <0.001). The numbers in parenthesis are relative energies in kJ/mol. The charges on Li in the most stable isomers of •GlyGly and GlyGly• are 0.532 (left)/0.532 (right) in the former and 0.544/0.493 in the latter.

(Table 1) and dipeptides with different residues were carried out (Table 2). The additional dipeptides used, are PheAla, AlaPhe, TrpAla and AlaTrp.

The $[GlyGly^{\bullet} + Li]^+$ precursor ion loses a 17-u neutral to form the fragment at *m/z* 121; this reaction could involve NH_3 or •OH radical loss. In the MS^3 spectrum of the corresponding d_4-isotopomer (Table 1) *m/z* 121 shifts entirely to *m/z* 122, indicating the loss of a 20-u neutral which is consistent only with ND_3. Ammonia is lost exclusively from the monolithiated C-terminal GlyGly• radical (Scheme 1). $[GlyGly^{\bullet} + Li]^+$ coproduces ions at *m/z* 82 and 80 (Fig. 5b); the mechanisms proposed for their formation are outlined in Scheme 2. The ion at *m/z* 82 is assigned the structure $[b_1 + OH + Li]^+$ [20,28–32], resulting from fragmentation through a mixed anhydride, similar to the

Table 1
CAD (MS^3) mass spectra of mono- and dilithiated •GlyGly and GlyGly•,[a] in which 3–4 heteroatom-bound (exchangeable) H atoms were replaced with D atoms

Distonic ion	*m/z* and Relative abundance (%)[b]			
d_3-$[^{\bullet}GlyGly + Li]^+$ (*m/z* 141)[c]		*m/z* 84	*m/z* 82	
		100	10	
d_4-$[GlyGly^{\bullet} + Li]^+$ (*m/z* 142)[d]	*m/z* 122	*m/z* 85	*m/z* 82	
	100	33	15	
d_3-$[^{\bullet}GlyGly - H + 2Li]^+$ (*m/z* 147)[d]	*m/z* 90	*m/z* 87	*m/z* 72	*m/z* 58
	30	100	50	33
d_3-$[GlyGly^{\bullet} - H + 2Li]^+$ (*m/z* 147)[d]	*m/z* 127	*m/z* 87		*m/z* 58
	100	40		5

[a] Produced via CAD of mono- and dilithiated PheGly and GlyPhe, respectively.
[b] Peak intensity relative to the base peak (from peak areas).
[c] All heteroatom-bound H atoms, except C-terminal COOH, exchanged with deuterium (see Section 2).
[d] All heteroatom-bound H atoms exchanged with deuterium.

Table 2
CAD (MS^3) mass spectra of mono- and dilithiated •GlyAla and AlaGly•

Dipeptide precursor	Distonic ion[a]	*m/z* and Relative abundance (%)[b]						
$[TrpAla+Li]^+$	$[^{\bullet}GlyAla+Li]^+$ (*m/z* 152)				*m/z* 96 100		*m/z* 79 81	*m/z* 50 [c]
$[PheAla+Li]^+$	$[^{\bullet}GlyAla+Li]^+$ (*m/z* 152)				*m/z* 96 100		*m/z* 79 78	*m/z* 50 33
$[TrpAla-H+2Li]^+$	$[^{\bullet}GlyAla-H+2Li]^+$ (*m/z* 158)		*m/z* 128 [c]	*m/z* 102 15	*m/z* 100 13	*m/z* 85 100	*m/z* 79 5	*m/z* 58 21
$[PheAla-H+2Li]^+$	$[^{\bullet}GlyAla-H+2Li]^+$ (*m/z* 158)		*m/z* 128 7	m/z 102 16	*m/z* 100 18	*m/z* 85 100	*m/z* 79 5	*m/z* 58 26
$[AlaTrp-H+2Li]^+$	$[AlaGly^{\bullet}-H+2Li]^+$ (*m/z* 158)	*m/z* 141 100				*m/z* 86 32		*m/z* 58 4
$[AlaPhe-H+2Li]^+$	$[AlaGly^{\bullet}-H+2Li]^+$ (*m/z* 158)	*m/z* 141 100				*m/z* 86 27		*m/z* 58 6

[a] Produced via CAD of the dipeptide precursor shown in the same row.
[b] Peak intensity relative to the base peak (from peak areas).
[c] At noise level.

one shown by Gronert and coworkers to occur in the closed-shell $[GlyGly+Li]^+$ complex [32]; the $[b_1+OH+Li]^+$ structure has three exchangeable hydrogens, which is corroborated by the *m/z* shift observed with d_4-$[GlyGly^{\bullet}+Li]^+$ (Table 1). The lithiated 2,3-dehydroglycine fragment (*m/z* 80; Scheme 2), on the other hand, has just two exchangeable protons, in agreement with its shift to *m/z* 82 with the deuterated isotopomer (Table 1). The latter ion is the product of a radical-induced bond scission. It is noteworthy that the isomeric $[^{\bullet}GlyGly+Li]^+$ complex does not undergo such a homolytic bond scission, possibly because a high energy N-centered radical [33] would be formed in this process. The dissociation $[GlyGly^{\bullet}+Li]^+ \rightarrow$ *m/z* 80 releases the acyl radical $H_2NCH_2CO^{\bullet}$. Such species easily lose CO [34], which might explain the minuscule abundance of the complementary fragment $[H_2NCH_2CO^{\bullet}+Li]^+$ (*m/z* 65) in the MS^3 spectrum (Fig. 5b).

For the $[^{\bullet}GlyGly+Li]^+$ precursor ion, as stated previously, different product ions are detected (Fig. 5). Tables 1 and 2 show, respectively, the product ions generated in the MS^3 experiments from d_3-$[^{\bullet}GlyGly+Li]^+$ and $[^{\bullet}GlyAla+Li]^+$. The procedure used to create d_3-$[^{\bullet}GlyGly+Li]^+$ (see Section 2) introduces D atoms mainly at the N-terminus and the amide nitrogen of this ion, cf. Fig. 3. The *m/z* 82 fragment from $[^{\bullet}GlyGly+Li]^+$ (Fig. 5a) shifts to *m/z* 84 with the d_3-isotopomer (Table 1) and to *m/z* 96 with the $[^{\bullet}GlyAla+Li]^+$ homolog (Table 2); these observations agree well with *m/z* 82 having a C-terminal y_1* ion structure (Scheme 3). The y_1* ion could be formed by C–N scission of the amidic peptide bond with synchronous 1,4-hydrogen rearrangement (1,4-*r*H) to release $HN{=}CH^{\bullet}+CO$, as depicted in Scheme 3. This mechanism is very similar to that established computationally and experimentally for the formation of $y_1+CO+HN{=}CH_2$ from protonated GlyGly [35,36].

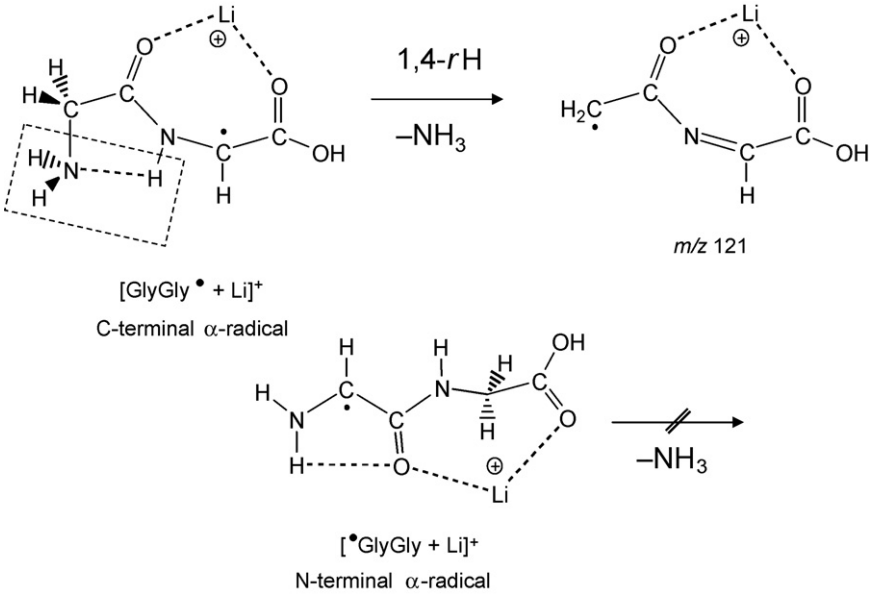

Scheme 1. Ammonia loss from lithiated GlyGly•. The Li^+ complex of the isomeric •GlyGly radical does not undergo this reaction upon CAD.

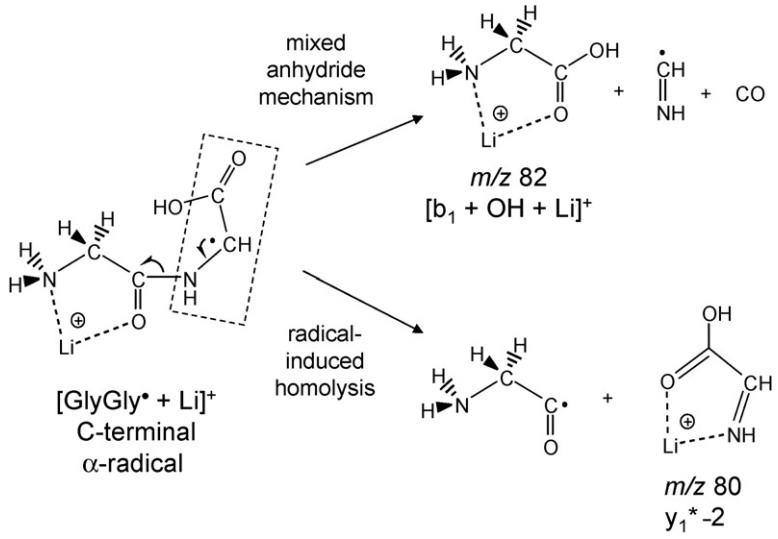

Scheme 2. Backbone fragmentations of lithiated GlyGly•. The mixed anhydride channel proceeds via the intermediate anhydride $H_2NCH_2C(=O)–O–C(=O)•CHNH_2$ and leads to the expulsion of the moiety encased in the rectangle. Fishhooks indicate the pathway of the radical-induced β-scission, which leads to the elimination of $H_2NCH_2CO•$.

Alternatively, the y_1* ion could arise through a mixed anhydride intermediate [20,32], as explained above for the $[b_1 + OH + Li]^+$ fragment from the $[GlyGly• + Li]^+$ isomer. Either mechanism is consistent with the labeling data.

The mixed anhydride mechanism converts the dipeptide GlyGly into the anhydride $H_2N–CH_2–C(=O)–O–C(=O)–CH_2–NH_2$, in which sequence information is compromised [32]. From the isomeric peptide radicals $[•GlyGly + Li]^+$ and $[GlyGly• + Li]^+$, the same mixed anhydride would be formed, viz. $H_2N–CH–C(=O)–O–C(=O)–•CH–NH_2$. This anhydride was invoked to explain the *m/z* 82 ion from $[•GlyGly + Li]^+$ as well as $[GlyGly• + Li]^+$. Besides *m/z* 82 ($[Gly + Li]^+$), the mixed anhydride could also generate *m/z* 81 ($[Gly• + Li]^+$) (see Scheme 1 in [20]). The latter product is not observed, however, presumably because of the significantly lower basicity and, hence, Li^+ binding energy of Gly• radical versus the Gly molecule.

Lithiated •GlyGly also forms a product ion at *m/z* 79 (Fig. 5a). The *m/z* value of this ion increases by 3 u with the deuterated isotopomer (Table 1) and remains unchanged with lithiated $[•GlyAla + Li]^+$ (Table 2); based on these facts, it can be concluded that 1,2-dehydroglycinamide (an N-terminal c_1* − 2 ion) is formed. A plausible pathway to such a fragment is included in Scheme 3 and involves homolytic scission of the N–C(COOH) bond accompanied by a H• rearrangement to release the carboxymethyl radical.

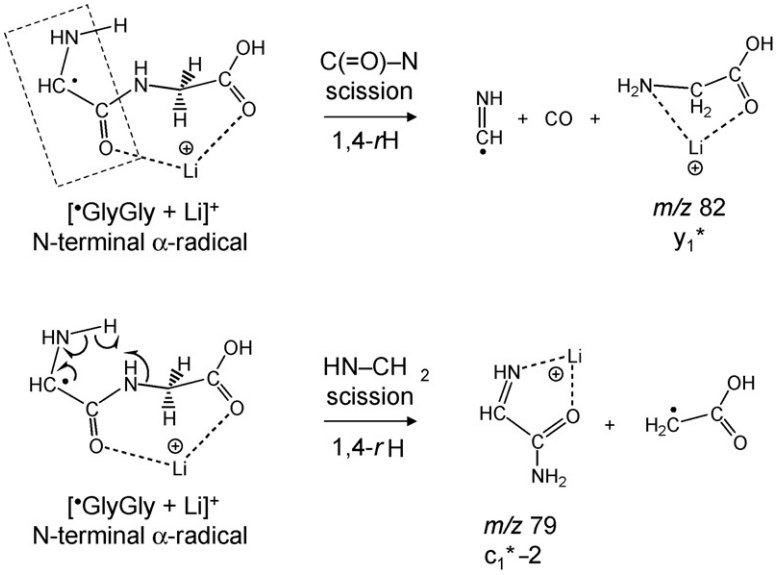

Scheme 3. Backbone fragmentations of lithiated •GlyGly.

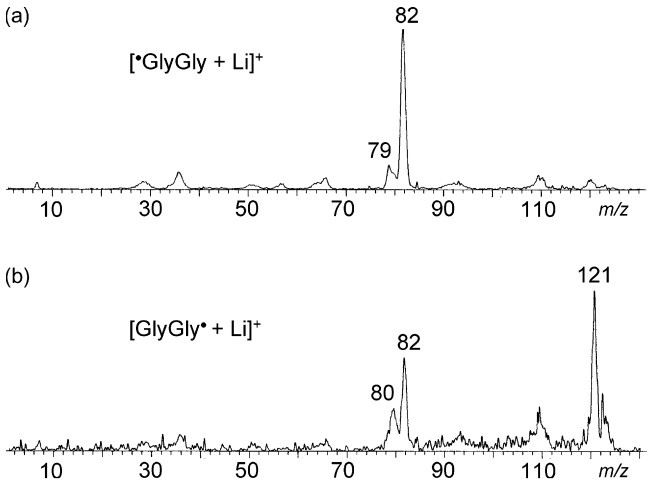

Fig. 5. CAD (MS^3) mass spectra of (a) $[^{\bullet}GlyGly + Li]^+$ and (b) $[GlyGly^{\bullet} + Li]^+$ (both at *m/z* 138). The numbers on top of the peaks give the corresponding mass-to-charge ratios.

3.4. Unimolecular chemistry of the dilithiated N- and C-terminal dipeptide radicals

Generation of distonic species (i.e. charged radicals) is observed from dilithiated dipeptides under CAD conditions as well, as already stated (Fig. 2). Their MS^3 (CAD/CAD) spectra are shown in Fig. 6 and document once again different unimolecular reactivities. To further characterize the product ions observed in the MS^3 spectra, multistage mass spectrometry experiments were performed on the deuterated isotopomers as well as on homologs containing Ala residues.

As with the monolithiated radicals, elimination of NH_3 (*m/z* 127) takes place only from the C-terminal radical complex. The only other significant fragment in the MS^3 spectrum of $[GlyGly^{\bullet} - H + 2Li]^+$ is *m/z* 86 (Fig. 6b). Experimental data suggest that this product ion is dilithiated 2,3-dehydro glycine (a $y_1^{**} - 2$ ion), produced from $[GlyGly^{\bullet} - H + 2Li]^+$ via direct C–N bond scission, as depicted in Scheme 4. This species has

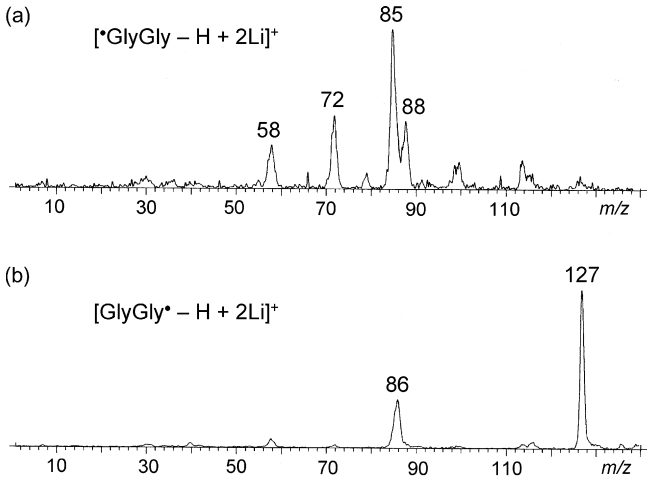

Fig. 6. CAD (MS^3) mass spectra of (a) $[^{\bullet}GlyGly - H + 2Li]^+$ and (b) $[GlyGly^{\bullet} - H + 2Li]^+$ (both at *m/z* 144). The numbers on top of the peaks give the corresponding mass-to-charge ratios.

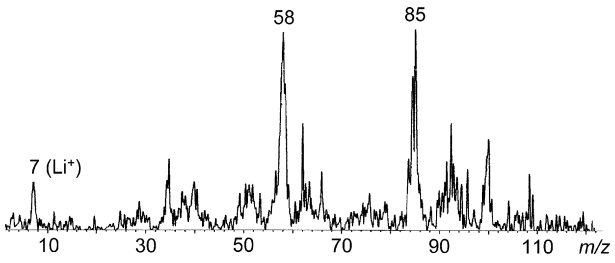

Fig. 7. CAD (MS^3) mass spectrum of the *m/z* 127 fragment generated by CAD (MS^2) of $[GlyPhe - H + 2Li]^+$ (see Fig. 2b). The numbers on top of the peaks give the corresponding mass-to-charge ratios.

one proton replaceable with deuterium, accounting for its *m/z* value of 87 from the d_3-isotopomer (Table 1). Dilithiated 2,3-dehydroglycine contains the C-terminal residue of dilithiated $GlyGly^{\bullet}$. As a result, it is also formed from the $AlaGly^{\bullet}$ distonic ion generated from dilithiated AlaTrp and AlaPhe (see *m/z* 86 in Table 2).

From the $[^{\bullet}GlyGly - H + 2Li]^+$ isomer, different fragments are formed upon CAD, the most prominent ones appearing at *m/z* 88, 85, 72 and 58 (Fig. 6a). The fragment with *m/z* 88 is the dilithiated glycine ion, a C-terminal fragment (y_1^{**} in Scheme 4). Supportive evidence for this structure is provided by the data shown in Tables 1 and 2. The deuterated isotopomer (Table 1) forms *m/z* 90 (two *m/z* units higher), consistent with C(=O)–N scission to form dilithiated glycine ion (y_1^{**}), after concomitant 1,4-proton rearrangement, as outlined in Scheme 4. Moreover, the MS^3 spectra of $[^{\bullet}GlyAla - H + 2Li]^+$ originating from TrpAla and PheAla (Table 2), show the expected shift to *m/z* 102, unequivocally proving that a C-terminal fragment is formed in this dissociation process. Similarly, the same set of MS^3 experiments decisively demonstrates that the basepeak at *m/z* 85 is dilithiated 2,3-dehydroglycinamide ($c_1^{**} - 2$ in Scheme 4). The D-labeling result (*m/z* 85 shifts to *m/z* 87, Table 1) agrees well with this structure. The mechanism proposed for the formation of this product ion involves N–CH_2 scission (Scheme 4), with concomitant hydrogen radical transfer from the N-terminal amine to a carboxylate oxygen to form a double bond and release the carboxymethyl radical. Note that dilithiated $^{\bullet}GlyAla$ also forms *m/z* 85 (Table 2), substantiating the N-terminal nature of this fragment. The other major product ions in the spectrum of Fig. 6a can be easily explained as dilithiated carboxymethyl ($^{\bullet}CH_2CO_2Li_2^+$, *m/z* 82) and carboxyl radicals ($^{\bullet}CO_2Li_2^+$, *m/z* 58).

Examination of the product ions from the dilithiated peptide radicals reveals that only C-terminal fragments are formed, when the α-radical site is at the C-terminal position. This fragmentation behavior is explainable, considering that $[GlyGly^{\bullet} - H + 2Li]^+$ undergoes ammonia loss extensively (Fig. 6b), destroying the N-terminal end. To further interrogate the structure of the product of NH_3 loss from $[GlyGly^{\bullet} - H + 2Li]^+$ (*m/z* 127), an MS^3 experiment was performed on the *m/z* 127 ion in the MS^2 spectrum of $[GlyPhe - H + 2\ Li]^+$ (Fig. 2b). The product ions of the MS^3 spectrum (Fig. 7) are consistent with the mechanism proposed in Scheme 5. The α-oxo methyl radical species formed after

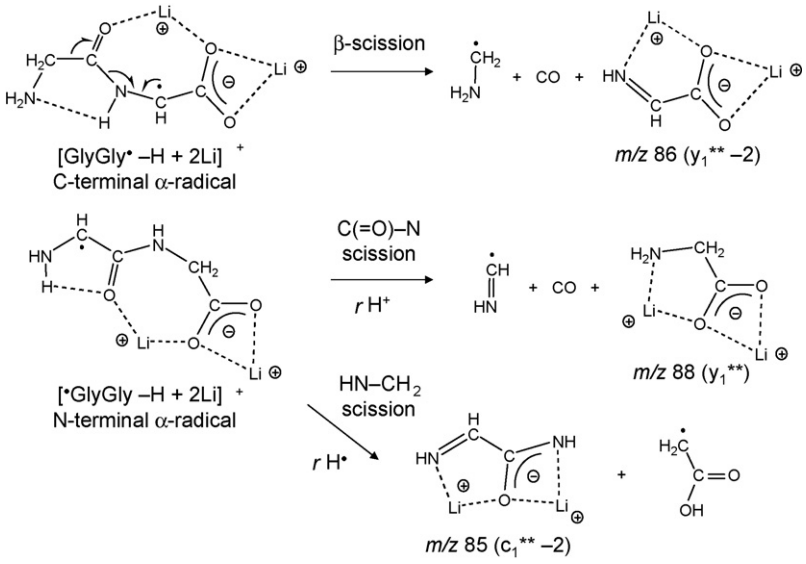

Scheme 4. Backbone fragmentations of dilithiated GlyGly• (top) and •GlyGly (center and bottom).

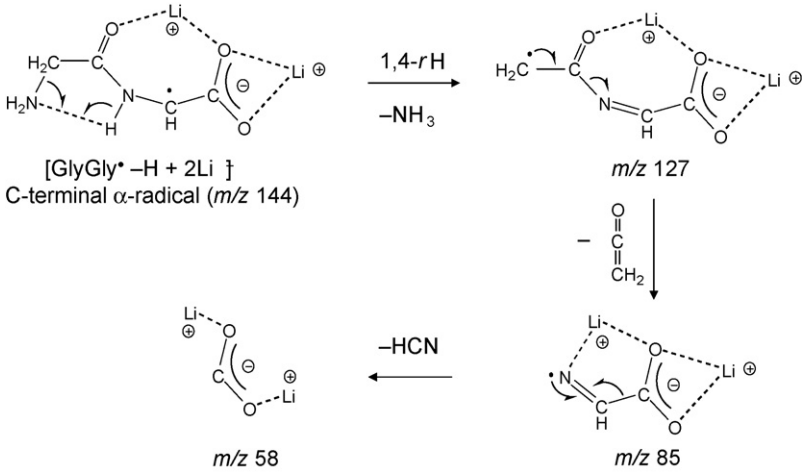

Scheme 5. Ammonia loss from dilithiated GlyGly• and consecutive fragmentation of the *m/z* 127 product ion via backbone cleavages releasing ketene and hydrogen cyanide.

ammonia loss (*m/z* 127) is proposed to release ketene to produce the dilithiated imine/carboxylate radical ion at *m/z* 85. The latter can undergo consecutive HCN elimination to ultimately yield dilithiated carboxyl radical ion (*m/z* 58).

Ammonia loss is unique to the mono- and dilithiated complexes carrying a C-terminal radical site, where the unpaired electron is in close proximity to the amidic hydrogen (Schemes 1 and 5). The radical site possesses electron deficient properties and, thus, exerts an electron-withdrawing effect which changes the electronic distribution of the amidic group, weakening the N–H bond. This in turn promotes the formation of a new bond to the amidic nitrogen by release of ammonia, a good leaving group.

4. Conclusions

Distonic radical ions derived from alkali metal ion complexes of dipeptides are of particular interest in Life Science, as such systems may also be formed from proteins in vivo, where alkali metal ions abound. Since dipeptide radical complexes contain the essential features and reactive sites of the larger protein radicals that have been implicated in a variety of biological processes, their stabilities and intrinsic reactivities, as determined by combining molecular orbital theory and tandem MS experiments, provide important clues as to how the larger protein systems may participate in radical reactions. Particularly interesting is the discovery that N- and C-terminal α-radical isomers do not interconvert (via a nominal 1,4-H rearrangement), but rather follow different channels of fragmentation.

Multistage mass spectrometry experiments were able to differentiate the structures of the isomeric α-dipeptide radical complexes studied. In order to establish the intrinsic chemical reactivities of these radicals, experiments with labeled isotopomers and with dipeptides having different amino acid sequences were necessary. With the combined experiments, it was possible to elucidate the favored dissociation pathways of

the isomers and establish the structures of their major fragments. Of special interest is the finding that both mono- and dilithiated C-terminal radical systems lose NH_3, while this loss is impeded in the N-terminal radical isomers due to the proximity of the radical site to the amine group. Although the experiments provided a wealth of information, in order to understand and characterize the intrinsic chemistry of the species under study, the parallel calculations were essential for unveiling the energetically favorable geometries of these species and their relative thermodynamic stabilities, and for confirming their distonic nature. The unimolecular reactions observed agree well with the computationally predicted most stable structures, and all major fragments can be generated from these structures with minimal reorganization.

Acknowledgements

This project was supported by the National Science Foundation. We thank Omnova Solutions Inc. for a graduate student fellowship to F.P. and the Ohio Board of Regents—Hayes Investment Fund for a grant to purchase the mass spectrometer used in this study. Dr. Jody M. Modarelli and Dr. Michael J. Polce are thanked for helpful discussions and experimental assistance.

References

[1] C.J. Easton, Chem. Rev. 97 (1997) 53.
[2] J. Stubbe, W.A. van der Dank, Chem. Rev. 98 (1998) 705.
[3] F. Minisci (Ed.), Free Radicals in Biology and Environment, Kluwer, Dodrecht, Netherlands, 1997.
[4] H.A. Headlam, A. Mortimer, C.J. Easton, M.J. Davies, Chem. Res. Toxicol. 13 (2000) 1087.
[5] C.L. Hawkins, M.J. Davies, J. Chem. Soc. Perkin Trans. 2 (1998) 2617.
[6] T. Yoshikawa, S. Toyokuni, Y. Yamamoto, Y. Naito (Eds.), Free Radicals in Chemistry, Biology and Medicine, OICA International Ltd., London, UK, 2000.
[7] X. Sun, S. Ollagnier, P.P. Schmidt, M. Atta, E. Mulliez, L. Lepage, R. Eliasson, A. Graeslund, M. Fontecave, P. Reichard, J. Biol. Chem. 271 (1996) 6827.
[8] F. Fieschi, E. Torrents, L. Toulokhonova, A. Jordan, U. Hellmann, J. Barbe, I. Gilbert, M. Karlsson, B.-M. Sjoberg, J. Biol. Chem. 273 (1998) 4329.
[9] J.B. Broderick, R.E. Duderstadt, D.C. Fernandez, K. Wojtuszewski, T.F. Henshaw, M.K. Johnson, J. Am. Chem. Soc. 119 (1997) 7396.
[10] R. Kulzer, T. Pils, R. Kappl, J. Huttermann, J. Knappe, J. Biol. Chem. 273 (1998) 4897.
[11] R.L. Smith, H.I. Kenttämaa, J. Am. Chem. Soc. 117 (1995) 1393.
[12] C.J. Petzold, L.E. Ramirez-Arizmedi, J.L. Heidbrink, J. Perez, H.I. Kenttämaa, J. Am. Soc. Mass Spectrom. 13 (2002) 192.
[13] C.J. Petzold, E.D. Nelson, H.A. Lardin, H.I. Kenttämaa, J. Phys. Chem. A 106 (2002) 9767.
[14] L.E. Ramirez-Arizmedi, J.L. Heidbrink, L.P. Guler, H.I. Kenttämaa, J. Am. Chem. Soc. 125 (2003) 2272.
[15] Y. Huang, H.I. Kenttämaa, J. Am. Chem. Soc. 125 (2003) 9878.
[16] L. Jing, L.P. Guler, J.L. Nash, H.I. Kenttämaa, J. Am. Soc. Mass Spectrom. 15 (2004) 913.
[17] J. Wu, M.J. Polce, C. Wesdemiotis, J. Am. Chem. Soc. 122 (2000) 12786.
[18] J.M. Talley, Ph.D. Dissertation, The University of Akron, December 2001.
[19] M.J. Polce, J.M. Modarelli, C. Wesdemiotis, Eur. J. Mass Spectrom. 10 (2004) 909.
[20] F. Pingitore, C. Wesdemiotis, Anal. Chem. 77 (2005) 1796.
[21] P. Wang, M.J. Polce, C. Bleiholder, B. Paizs, C. Wesdemiotis, Int. J. Mass Spectrom. 249/250 (2006) 45.
[22] I.K. Chu, C.F. Rodriquez, T.-C. Lau, A.C. Hopkinson, K.W.M. Siu, J. Phys. Chem. B 104 (2000) 3393.
[23] E. Bagheri-Majdi, Y. Ke, G. Orlova, I.K. Chu, A.C. Hopkinson, K.W.M. Siu, J. Phys. Chem. B 108 (2004) 11170.
[24] I.K. Chu, S.O. Siu, C.N.W. Lam, J.C.Y. Chan, C.F. Rodriquez, Rapid Commun. Mass Spectrom. 18 (2004) 1798.
[25] C.K. Barlow, W.D. McFadyen, R.A.J. O'Hair, J. Am. Chem. Soc. 127 (2005) 6109.
[26] M.J. Frisch, Gaussian-98, Rev. A9, Gaussian Inc., Pittsburgh, 1995.
[27] R.C. Dunbar, J. Phys. Chem. A 104 (2000) 8067.
[28] R.P. Grese, M.L. Gross, J. Am. Chem. Soc. 112 (1990) 5098.
[29] L.M. Teesch, J. Adams, J. Am. Chem. Soc. 113 (1991) 812.
[30] J.M. Barr, M.J. Van Stipdonk, Rapid Commun. Mass Spectrom. 16 (2002) 566.
[31] M.M. Kish, C. Wesdemiotis, Int. J. Mass Spectrom. 227 (2003) 191.
[32] W.Y. Feng, S. Gronert, K.A. Fletcher, A. Warres, C.B. Lebrilla, Int. J. Mass Spectrom. 222 (2003) 117.
[33] D.F. McMillen, D.M. Golden, Ann. Rev. Phys. Chem. 33 (1982) 493.
[34] R. Mereau, M.-T. Rayez, J.-C. Rayez, F. Caralp, R. Lesclaux, Phys. Chem. Chem. Phys. 3 (2001) 4712.
[35] B. Paizs, S. Suhai, Rapid Commun. Mass Spectrom. 15 (2001) 651.
[36] B. Paizs, S. Suhai, Mass Spectrom. Rev. 24 (2005) 508.